JOURNAL OF MATERIALS SCIENCE 27 (1992) 671–674

Structural stability and stacking faults in a laser-melted ZL108 Al–Si alloy containing rare earth

HU JIANDONG
Senior Engineer, Microanalysis Center, Jilin University of Technology, Changchun, 130025, People's Republic of China

The ZL108 Al–Si alloy containing rare earth was melted with a CO_2 2 kW laser. The maximum microhardness values of the laser-melted zone (LMZ) was shifted back by 2 h in the microhardness–time curve and 20 °C in the microhardness–temperature curve, as compared with conventional treatment materials in the given range. The LMZ had better structural stability at the elevated temperature than that of the conventional materials. Stacking faults were found in the resolidified aluminium, and were identified to be intrinsic. Both structural stability and the existence of the stacking faults were related to Ce supersaturation in the resolidified aluminium.

1. Introduction

Aluminium alloys have frequently been used for surface melting and have a number of industrial applications in pistons, liners, bearing impellers, bushings and machine shrouds. Thus significant interest has developed in the laser processing of aluminium [1, 2]. Laser processing is a typical kind of surface treatment because the melting layer is usually confined within 1 mm depth. Element redistribution in the laser-melted zone can be achieved by rapid heating and cooling. This leads to many changes in the microstructure of laser-melted materials. One example is the finding of pearlite-like aluminium–silicon eutectic in the laser-melted ZL108 aluminium–silicon alloy [3]. Further to our previous work, in this paper we study the influence of laser melting on elevated temperature properties and microstructure. Some new findings such as stacking faults are reported. The reason for the existence of stacking faults is also discussed.

2. Experimental procedure

The material used was ZL108 Ai–Si alloy made in China. Its chemical composition was 12 wt % Si, 1.23 wt % Cu, 1.0 wt % Mg, 0.5 wt % Mn and 0.10 wt % rare earth (Al balance). The rare earth contained 10 wt % Ce. Specimens with size $50 \times 50 \times 100$ mm were mounted on a numerically controlled x–y table and irradiated with a CO_2 laser, model HGL–81 using single passes. Laser melting was achieved by traversing the specimens at a speed of 7.5 mm s^{-1} using a power of 1.2 kW. The laser beam was focused on a spot 3.5 mm in diameter. The specimens processed were divided into two groups, one of which was aged at 200 °C for 2, 4, 6, 8 and 10 h, respectively. The other group was aged for 6 h at temperatures of 160, 180, 200, 220 and 240 °C. Specimens treated conventionally were employed as a standard, heated at 515 °C for 8 h, followed by quenching into water. Both laser-processed and conventionally treated specimens were aged under the same conditions. The microhardness of the specimens was measured using a load of 50 g. Each microhardness value reported here is an average value of nine measurements.

Slices prepared for thin foils were mechanically cut along the longitudinal direction parallel to the direction of the specimen surface processed. After having been thinned using a series of SiC papers, the slices were machined by dual ion milling to a thickness which was electron transparent. The thin foils were examined in a H-800 transmission electron microscope (TEM), operated at a voltage of 200 kV.

3. Results

3.1. Structural stability of the laser-melted zone

The influence of ageing time and temperature on microhardness was studied. Fig. 1a shows microhardness varying with ageing time (at 200 °C). The microhardness of the laser-melted zone (LMZ) is higher than that of conventional treatment materials in the whole range. The maximum microhardness value (136 HV) for the LMZ is at 6 h, 2 h longer than that (122 HV) for the conventional treatment materials. Fig. 1b shows microhardness as a function of ageing temperature. The maximum microhardness value of the LMZ moves towards the higher temperature by 20 °C as compared with the conventional materials. It is noted that in comparison with the LMZ, there is a great drop in microhardness for the CTM with increasing ageing temperature. This makes

0022–2461/92 $03.00 + .12

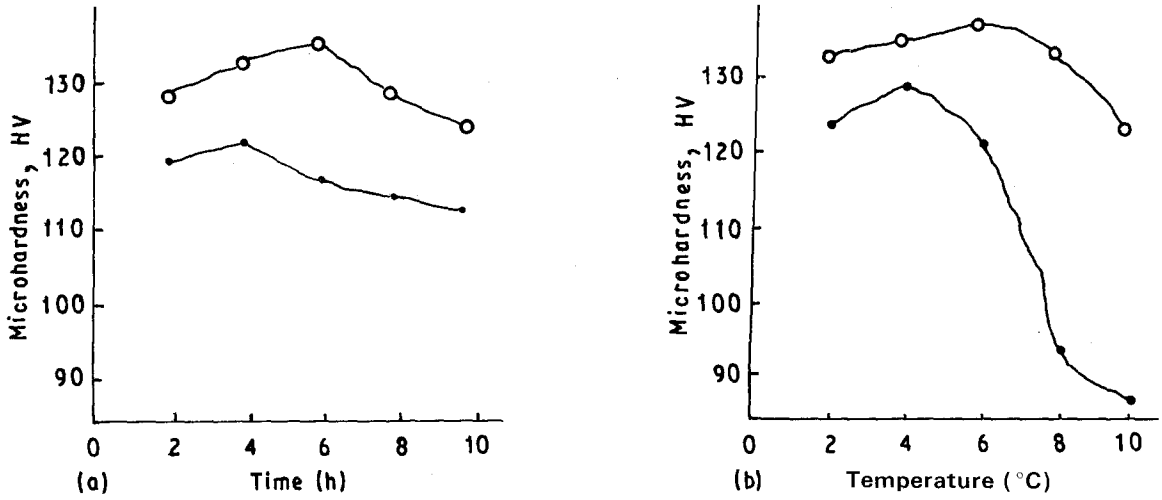

Figure 1 Influence of ageing time and temperature on microhardness. (a) Microhardness against ageing time; (b) microhardness against ageing temperature. ○, LMZ; ●, conventional treatment materials.

the difference in microhardness become obvious at 180 °C for 6 h. Thus the LMZ has better high-temperature strength than conventional treatment materials.

3.2. Microstructure

Fig. 2a, b shows metallographs for the LMZ. An ultrafine dendritic structure was obtained, and the secondary arm spacing is up to 2 μm. The interface between LMZ and substrate can be seen in Fig. 2b. The upper part of the micrograph represents the LMZ, the lower part the substrate. This indicates that the LMZ yields a refined dendritic structure owing to a high solidification rate. Draper [4] reports the

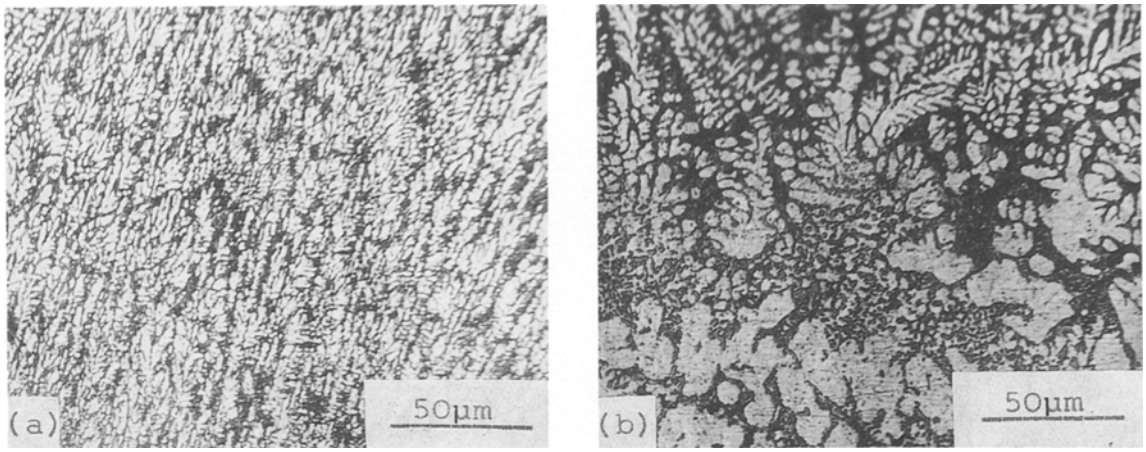

Figure 2 SEM of laser-melted zone, showing eutectic and aluminium dendrite. (a) Upper melted region; (b) lower melted region, showing interface between laser-melted zone and matrix.

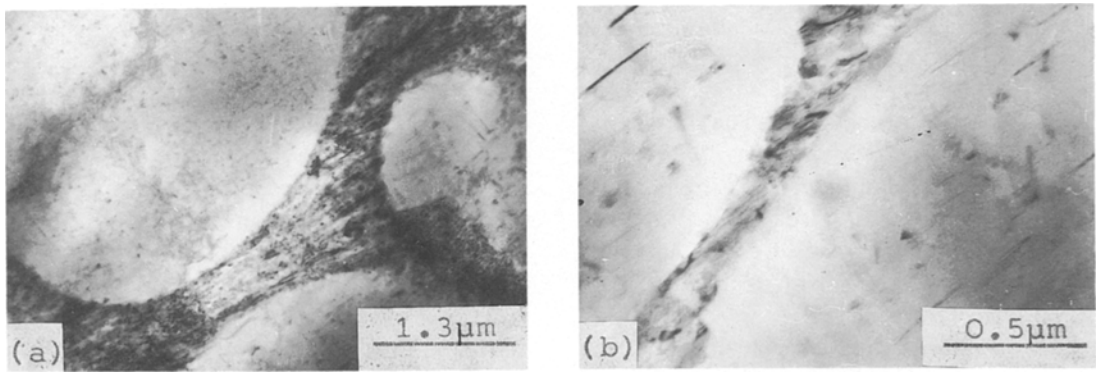

Figure 3 TEM micrographs, showing primary aluminium crystals and eutectic in the laser-melted zone, aged at 200 °C for 6 h. (a) Primary aluminium crystals and eutectic; (b) high magnification of (a), showing θ″ phases in two neighbouring primary aluminium crystals.

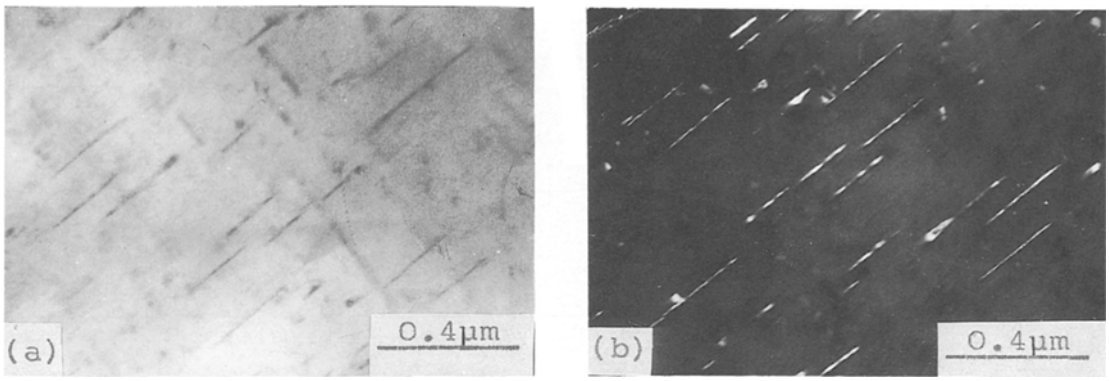

Figure 4 TEM micrographs showing θ″ phases aged at 200 °C for 6 h. (a) Bright field; (b) dark field.

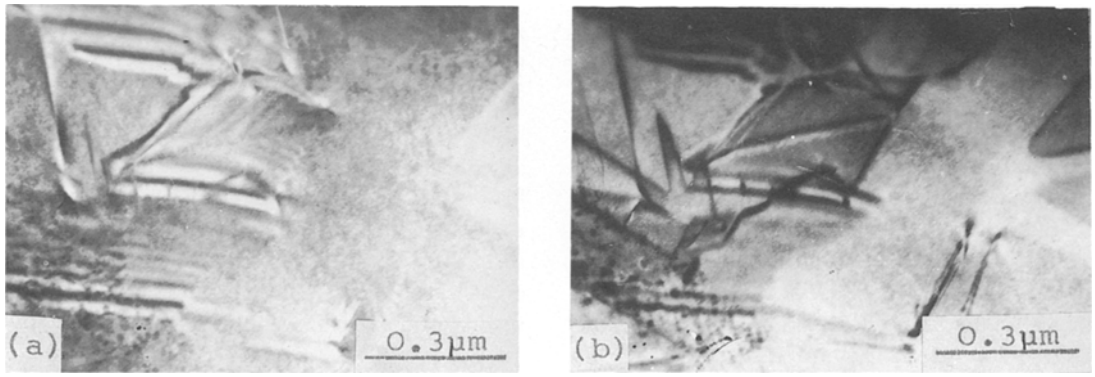

Figure 5 TEM micrographs of the resolidified aluminium aged at 200 °C for 6 h. (a) Bright field micrograph of several stacking faults; (b) dark field micrograph.

cooling rate of laser-processed materials to be more than 10^4 °C s^{-1}. Munitz [1] points out that the cooling rate of a laser-melted Al–4.5 wt % Cu alloy was calculated to be 10^5 °C s^{-1}, in the case of SDA up to 1.3.

Fig. 3a, b shows the resolidified aluminium crystals and eutectic for the LMZ after ageing at 200 °C for 6 h. The eutectic is a pearlite-like structure with a crystallographic relationship of [1 1 0] Si ∥ [0 0 1] Al, and [1 1 1] Si ∥ [1 0 0] Al [3].

The growth direction of the aluminium crystal was recognized to be the {0 0 1} direction. θ″ phases ($a = b = 0.40$ nm and $c = 0.77$ nm) were precipitated in the aluminium, lying on [0 0 1] basal planes. It is seen that the Q'' precipitates which formed in the two neighbouring crystals remain in the same direction as in Fig. 3b. Fig. 4a, b shows the θ″ precipitates in detail, which are seen to form on the [0 1 0] crystal face of the aluminium. It is interesting to note that the θ″ precipitates as found in the LMZ were observed in the conventional treatment materials after ageing at 200 °C for 4 h. These are in agreement with the peak values shown in Fig. 1a. Thus it is concluded that the precipitation of the θ″ is related to the maximum microhardness values.

3.3. Stacking faults

Fig. 5a, b shows the stacking faults for the resolidified aluminium using the 0 0 2 reflection to image the dark field. The stacking faults are bounded by partial dislocations. Using the method of Hashimoto *et al.* [5] all of the faults were determined to be intrinsic.

4. Discussion

The fact that the microhardness of the LMZ is higher than that of the conventional treatment materials in any given range is responsible for the refined structure. Both LMZ and conventional treatment materials show microhardness going through the maximum values in the curves; however their maximum values are different. This cannot be explained by the effect of the refined structure. Furthermore, the microhardness of the LMZ is slightly reduced with increasing ageing temperature, as compared with the LMZ. This cannot be related only to the structural change produced by laser melting. Thus we must consider this problem in another way. Cu redistribution in the laser-melted alloy has been reported [6]. Table I shows the results. It is seen that no significant concentration of Cu occurred, except for a slight drop at the interface. It is difficult to detect Ce distribution in the LMZ quantitatively. However, a qualitative result (Table II) was done in an earlier experiment [7].

It is seen that Ce in the LMZ becomes more homogeneous than in the substrate. The redistribution of some elements can be improved, which will bring about changes in microstructure. The θ″ phase is known to serve as an effective precipitation strengthener [8], as it undergoes a process of formation from GP zone → θ″ → θ′ → θ during ageing. Rapid heating

TABLE I Copper concentration related to distance from the surface

	Laser-melted zone						Interface		Substrate
Copper concentration (wt%)	1.22	1.20	1.23	1.25	1.22	1.24	1.02	1.12	1.22
Distance from surface (mm)	0.1	0.2	0.3	0.4	0.5	0.6	0.7	0.8	0.9

TABLE II Ce distribution

Measurements	1	2	3	4	5	6	7	8	9
LMZ (cps)	Yes	No	Yes	Yes	Yes	Yes	Yes	Yes	Yes
Substrate (cps)	No	Yes	No	Yes	No	No	No	Yes	No

and solidification rates for the LMZ can be achieved when melted. This enhances the solubility of Ce in the aluminium. Rare-earth elements have many special characteristics such as active chemical properties, high specific gravity and large radius, and many minus charges in the nucleus. Ce atoms become ions when soluted. Thus electrons cannot maintain electronic equilibrium. In this case, electron distribution appears to be inhomogeneous so that some local areas have a strong negative electrical force. This decreases the diffusion rate of copper atoms and postpones GP zone formation at relatively high temperatures or long times. Thus, Ce supersaturation is thought to be responsible for the good structural stability of the LMZ at elevated temperatures.

Aluminium and its alloys have been known to have high stacking fault energy, so that it is difficult to discover stacking faults in them. It has been reported that stacking fault energy decreases with increasing electron density [9]. Thus the likely reason for the existence of the stacking fault is that electron density increases, resulting from Ce supersaturation in the resolidified aluminium.

5. Conclusions

The microhardness of both LMZ and conventional treatment materials have maximum values with increasing ageing time or temperature. However, the maximum value for the LMZ shifts back by 2 h in the microhardness–time curve, and 20 °C in the microhardness–temperature curve, as compared with the conventional treatment materials, and the microhardness of the LMZ is slightly reduced with increasing ageing temperature. This indicates that the LMZ has better high-temperature strength. The existence of the maximum values is related to θ'' phase precipitation formed in the resolidified aluminium. The LMZ becomes supersaturated with Ce as a result of laser melting. This decreases the rate of Cu diffusion and θ'' formation. Ce supersaturation in the aluminium increases the electron density in the local areas and results in decreasing stacking fault energy.

Acknowledgements

The author thanks Professor Du Waixi for supplying the as-cast specimens, and Dr Liu Yongbing for many fruitful discussions.

References

1. A. MUNITZ, *Metall. Trans.* **16B** (1985) 149.
2. J. M. BROWN and J. A. SEKHAR, *ibid.* **15A** (1984) 29.
3. HU JIANDONG, LIU YONGBING and LI ZHANG, *J. Mater. Sci. Lett.* **9** (1990) 587.
4. C. W. DRAPER, *J. Metals* **34** (1982) 24.
5. H. HASHIMOTO, A. HONIE and M. J. WHELAN, *Proc. R. Soc. A* **269** (1962) 80.
6. HU JIANDONG and LI ZHANG, *Trans. Met. Heat Treat.* **10** (1989) 95 (in Chinese).
7. *Idem, Rare Earth* **3** (1987) 7 (in Chinese).
8. M. G. SCOTT and J. A. LEAKE, *Acta Metall.* **23** (1975) 503.
9. P. R. THORNTON, T. E. MICHELL and P. B. HIRSH, *Phil. Mag.* **7** (1962) 1349.

Received 3 October 1990
and accepted 20 March 1991